Dark matter signatures around dirty black hole binaries

@ New horizons for Psi

Instituto Superior Tecnico
Lisbon, 5 July 2024

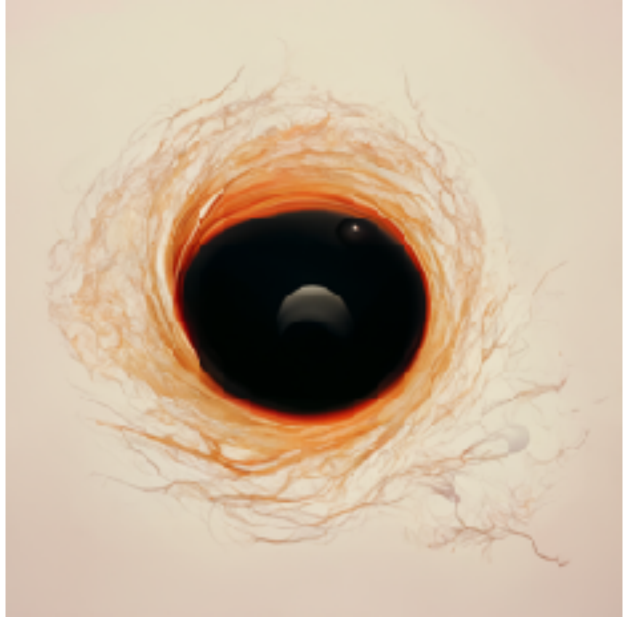

Andrea Maselli

GRAN SASSO SCIENCE INSTITUTE
SCHOOL OF ADVANCED STUDIES
Scuola Universitaria Superiore

Why so dusty?

GW sources evolve in a variety of gas/matter contents/fields, which may leave detectable imprints on GW ⟶ *changes in generation and propagation of GWs*

- Can we infer properties on the environment in which binaries evolve?
- Are vacuum templates safe against (astrophysical) systematics?

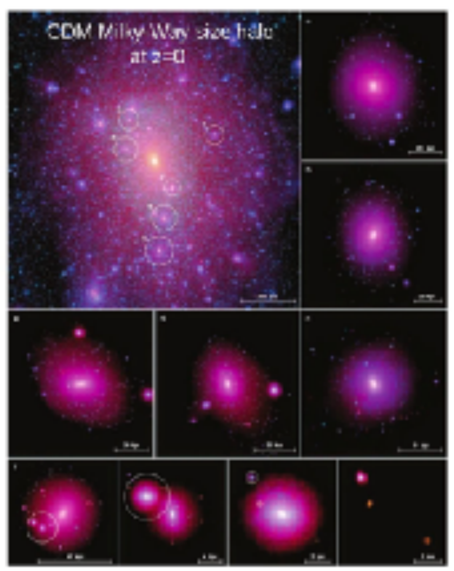

V. Springel et al., Mon. Not. Roy. Astron. 391 (2008)

G. Bertone et al., Nature 562, 7725 (2008)

massive BH evolve in DM-rich environment, within galaxies

binaries can assemble and evolve in accretion disks

theoretical arguments supporting new fields clustering at different scales

....

Dusty phase shifts

The environment affects the binary orbital motion

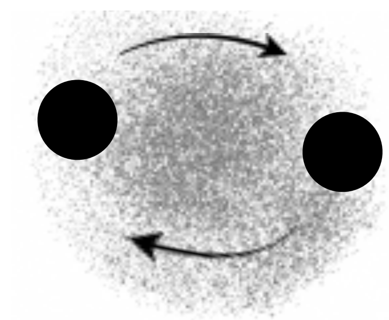

→ *changes generation and propagation of GWs*

- different effects can be included adding specific corrections the post-Newtonian waveforms $h = Ae^{i\psi_{\rm GW}}$

Cardoso & Maselli AA 644, A147 (2020)

$$\psi_{\rm GW} \propto (m\pi f)^{-5/3}\left[vacuum + \delta\psi_{\rm env}\right]$$

- generic correction due to the binary environment

$$\delta\psi_{\rm env} \propto \rho_{\rm env}(\pi m f)^{-\gamma}$$

density of the medium

$\gamma = 11/3$ | $\gamma = 3$ | $\gamma = 2$

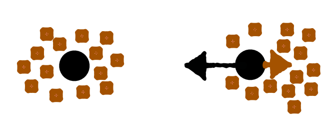

gravitational drag | *accretion* | *gravitational pull*

- GW can be used to bound the density of the matter distribution in which binary evolve

Where do we look for the dust

Constraints on the environment's density from different effects & sources & detectors

V. Cardoso & A. M., A&A 644, A147 (2020)

- environmental effects typically contribute at low frequencies

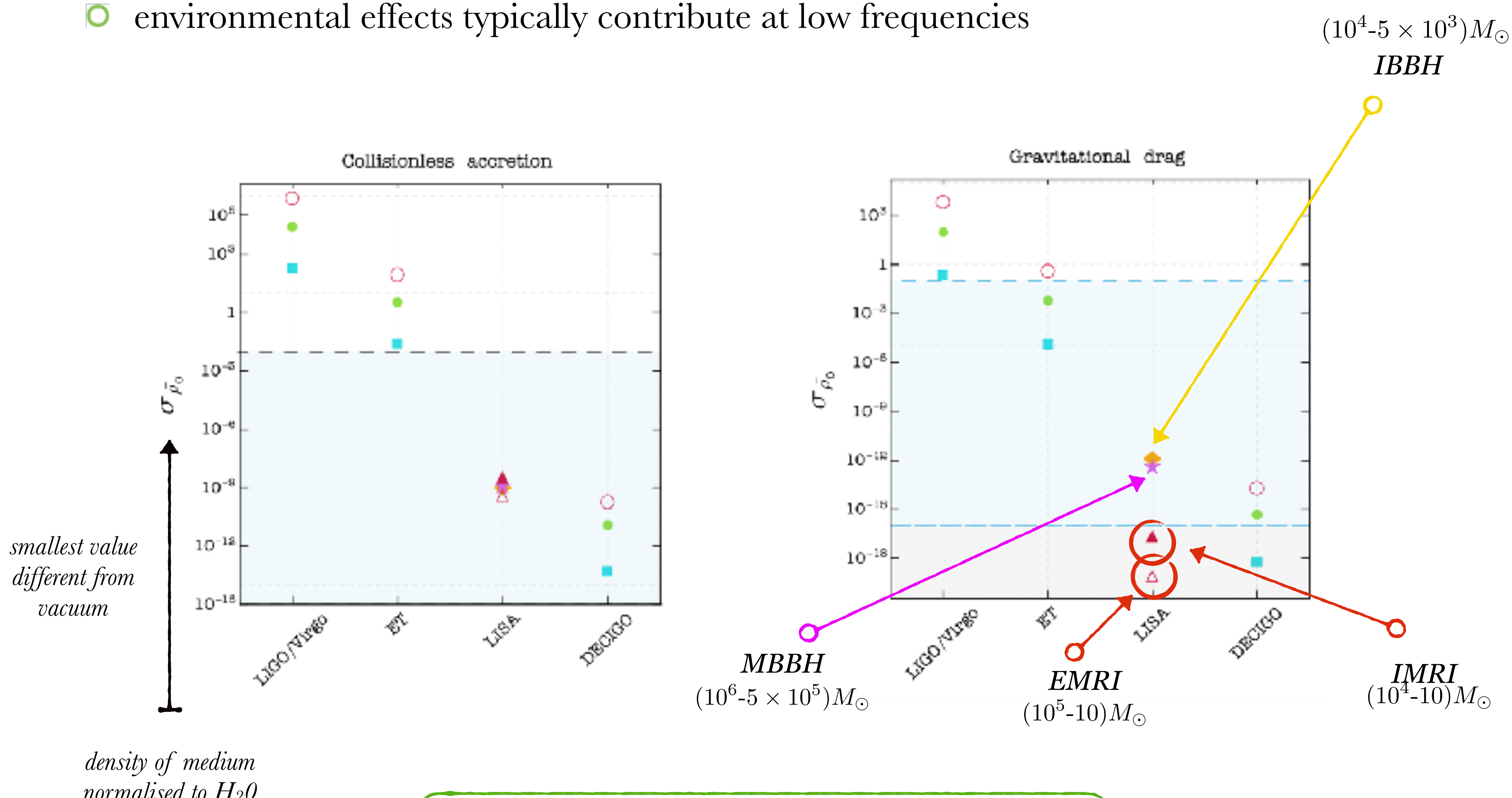

Asymmetric binaries work (really) well

EMRIs in nuce

EMRIs provide a rich phenomenology, due to their orbital features

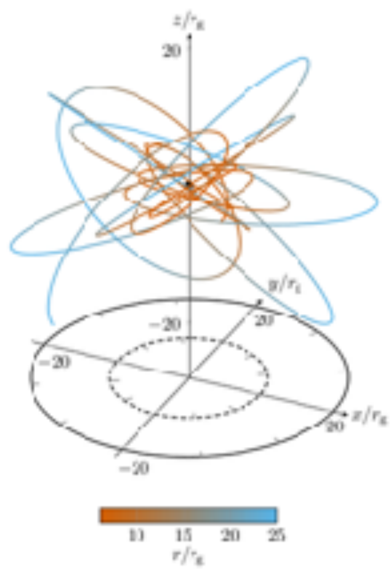

Berry +, Astro2020 1903.03686 (2019)

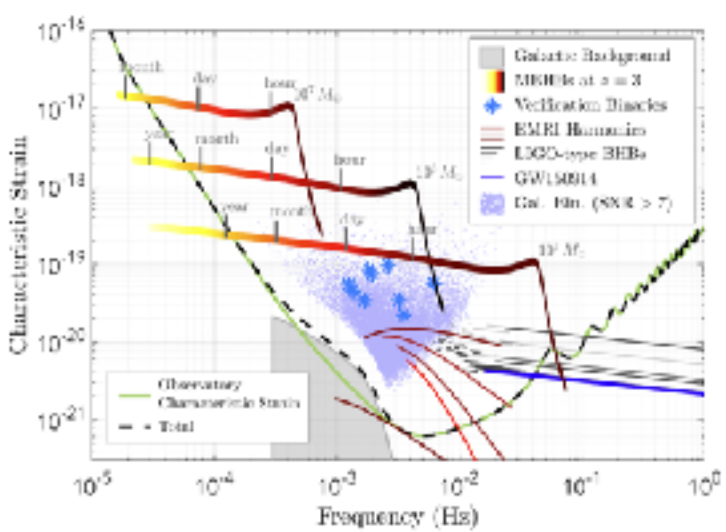

- Non equatorial orbits
- Eccentric motion
- Resonances
- Complete $\sim (10^4 - 10^5)$ cycles before the plunge

dynamics dictated by q

blessing & **disguise**

Tracking EMRIs for O(year) requires accurate templates

Very appealing to test fundamental & astro-physics

Precise space-time map and accurate binary parameters

How do we describe dusty BHs?

Different approaches to compute GW signals

$\tilde{h}(f) = Ae^{i\psi_{\rm GW}}$

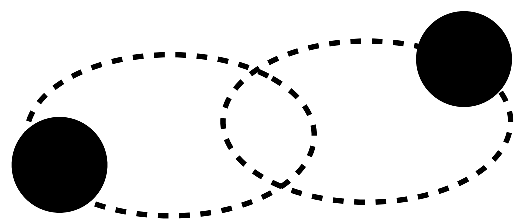

post-Newtonian theory

speed of light expansion $\frac{v}{c}$

$$\psi_{\rm GW} \propto (m\pi f)^{-5/3}\left[1 + \frac{(m\pi f)^{2/3}}{c^2} + \frac{\cdots}{c^3} + \cdots\right.$$

- breaks before the merger
- good for comparable mass binaries
- bad for asymmetric binaries

(some) dirty BH models

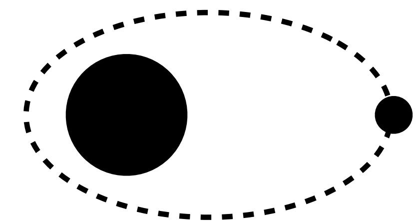

Self-Force theory

mass ratio expansion $q = \frac{m_2}{m_1} \ll 1$

$$\psi_{\rm GW} \propto \underset{\mathcal{O}(1/q)}{\underset{\downarrow}{\psi_{\rm 0PA}}} + \underset{\mathcal{O}(1)}{\underset{\downarrow}{\psi_{\rm 1PA}}} + \ldots$$

- fully relativistic
- good for asymmetric binaries
- bad for comparable mass binaries (but)

(almost) no dirty BH model

The Background

Solve Einstein's equations in spherical symmetry sourced by the halo stress-energy tensor

V. Cardoso + A. M., PRDL 105, L061501, (2022)
V. Cardoso + A. M., PRL 129, 241103, (2022)
E. Figueiredo, A. M., V. Cardos, PRD 107, 104033, (2023)

$$\rho(r) = \rho_0 (r/a_0)^{-\gamma}[1+(r/a_0)^{\alpha}]^{(\gamma-\beta)/\alpha} \qquad \rho(r) = \rho_e \exp\left\{-d_n[(r/r_e)^{1/n}-1]\right\}$$

Hernquist *NFW* *Einasto*

$$g_{rr}^{-1} = 1 - 2m(r)/r$$

$$g_{tt} = \left(1 - \frac{2M_{\rm BH}}{r}\right) e^{\Gamma} \xrightarrow[a_0\to\infty]{} 1 - 2M_{\rm halo}/a_0 \longleftarrow \textit{Redshift factor}$$

- Asymptotically flat, $r_h = 2M_{\rm BH}$
- To mimic galaxy observations

$$a_0 \gtrsim 10^4 M_{\rm halo} \longrightarrow M_{\rm BH} \ll M_{\rm halo} \ll a_0$$

- Model characterised by $M_{\rm halo}, a_0$

particle motion (geodesics)

"assemble" binaries and study GW emission

Spikes

The halo mass function

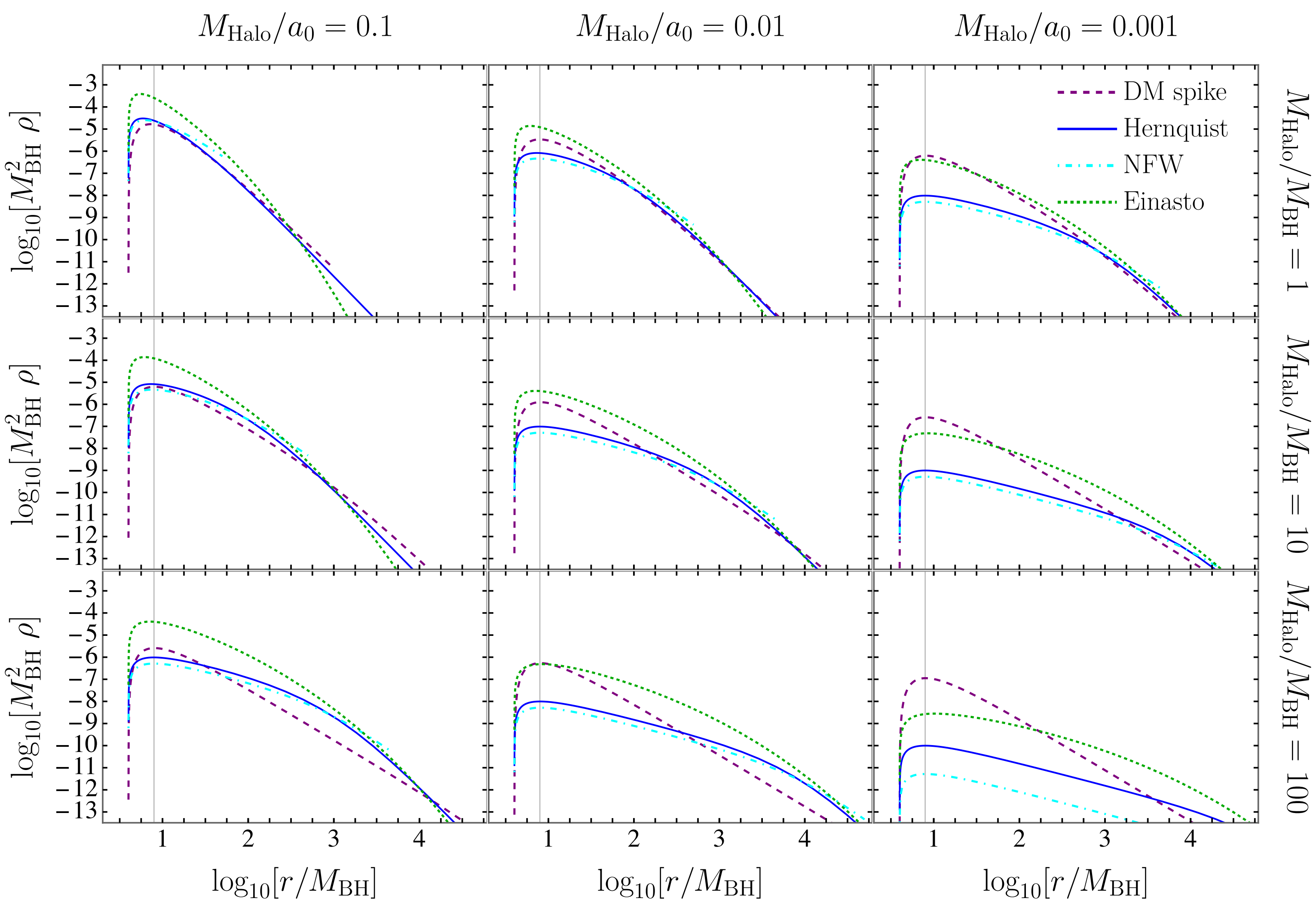

numerical simulations of BH accretion growth predict spikes with overdensities

P. Gondolo & J. Silk, PRL 83, (1999)

- lengthscale dependent on the BH mass
- spike vanishing at $4M_{\rm BH}$

- Spikes are relevant to enhance GW emission for close binaries and hence environment detectability

Spikes

The halo mass function

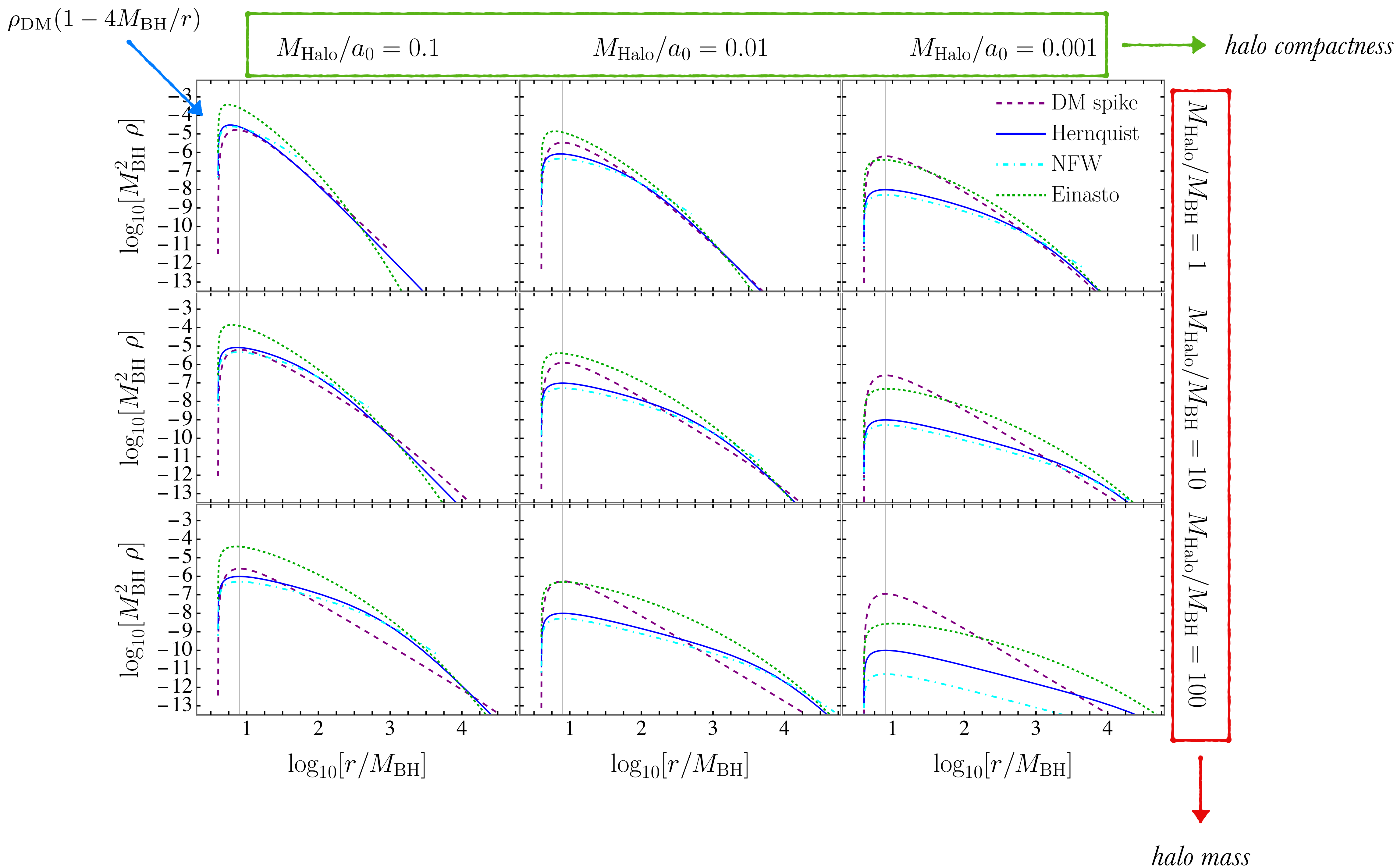

Geodesics

The halo affects the orbital properties of massive and massless particles

Innermost Stable Circular Orbit

Light Ring

$$M_{\rm BH}\Omega_{\rm ISCO} \simeq \frac{1}{6\sqrt{6}}$$

vacuum

$$M_{\rm BH}\Omega_{\rm LR} \simeq \frac{1}{3\sqrt{3}}$$

$$M_{\rm BH}\Omega_{\rm ISCO} \simeq \frac{1}{6\sqrt{6}}\left(1 - \frac{M_{\rm halo}}{a_0} + \text{non-linear corrections}\right)$$

redshift factor

$$M_{\rm BH}\Omega_{\rm LR} \simeq \frac{1}{3\sqrt{3}}\left(1 - \frac{M_{\rm halo}}{a_0} + \text{non-linear corrections}\right)$$

redshift factor

- At leading order the halo only redshifts the dynamics
- Non-linear correction of the order $M^2/a_0^2 \lesssim 10^{-8}$

GW emission from EMRI

EMRI evolving within environments

- Consider linear perturbations of a BH+halo background induced by the small secondary $\mathcal{G}_{\mu\nu} = 8\pi(T_{\mu\nu} + T^{p}_{\mu\nu})$

gravitational-sector

$$g_{\alpha\beta} = g^{(0)}_{\alpha\beta} + h^{\rm ax}_{\alpha\beta} + h^{\rm pol}_{\alpha\beta}$$

fluid-sector

$$u_\mu = u^0_\mu + u^1_\mu \qquad \rho = \rho_0 + \rho_1$$

- Compute GW fluxes $\dot{E}_{\rm GW} \sim |h^{\rm ax,pol}_{\mu\nu}|^2$

- Evolve orbital elements

orbital phase

orbital radius

$$\frac{dr(t)}{dt} = -\dot{E}_{\rm GW}\frac{dr}{dE_{\rm orb}} \qquad \frac{d\phi(t)}{dt} = \frac{M_{\rm BH}^{1/2}}{r^{3/2}}$$

Axial modes

How does the halo change the axial perturbations of the BH?

- Same functional as in vacuum

$$\frac{d^2 R_{\ell m}}{dr_\star^2} + [\omega^2 - V^{\rm ax}]R_{\ell m} = J_{\rm ax}$$

$$V^{\rm ax} = \frac{a(r)}{r^2}\left[\ell(\ell+1) - \frac{6m(r)}{r} + m'(r)\right]$$

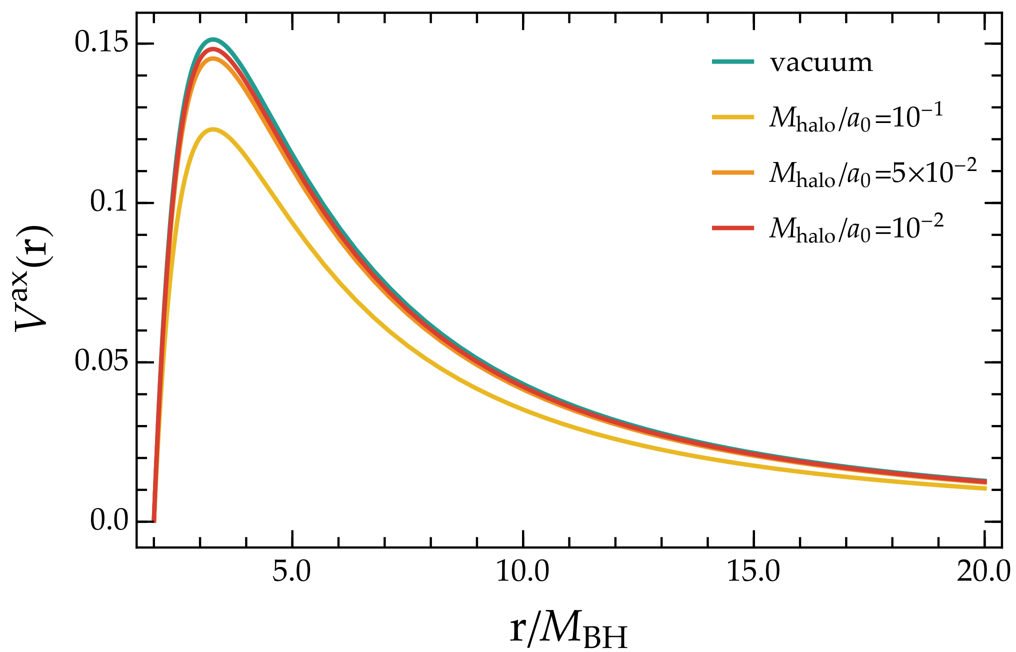

Change in the scattering potential due to the halo compactness

- The halo affects the structure of the potential and boundary conditions
- axial modes *are not* coupled to fluid perturbations

Redshift again

In the small compactness limit $M/a_0 \ll 1$

$$V^{\rm ax} \approx \left(1-\frac{2M_{\rm halo}}{a_0}\right) V^{\rm ax}_{\rm Schw} \qquad J^{\rm ax}_{\ell m} \approx \left(1-\frac{3M_{\rm halo}}{a_0}\right) J^{\rm ax,Schw}_{\ell m} \qquad \frac{dr}{dr_*} \approx \left(1-\frac{M_{\rm halo}}{a_0}\right)\frac{dr}{d\tilde{r}_*}$$

$$\frac{d^2\psi^{\rm ax}}{d\tilde{r}_*^2} + \left[\left[\omega\left(1+\frac{M_{\rm halo}}{a_0}\right)\right]^2 - V^{\rm ax}_{\rm Schw}\right]\psi^{\rm ax} = \left(1-\frac{M_{\rm halo}}{a_0}\right) J^{\rm ax,Schw}_{\ell m}$$

$$\Omega_p \to \tilde{\Omega}_p = \Omega_p\left(1-\frac{M_{\rm halo}}{a_0}\right)$$

$$\mu \to \tilde{\mu} = \mu\left(1+\frac{M_{\rm halo}}{a_0}\right)$$

Equivalent to a vacuum solution with rescaled parameters

redshift of the BH mass

Axial modes

(2,1) axial flux emitted by an EMRI on circular motion

E. Figueiredo, A. M., V. Cardos, PRD 107, 104033, (2023)

- fluxes tend to be smaller in the presence of the halo

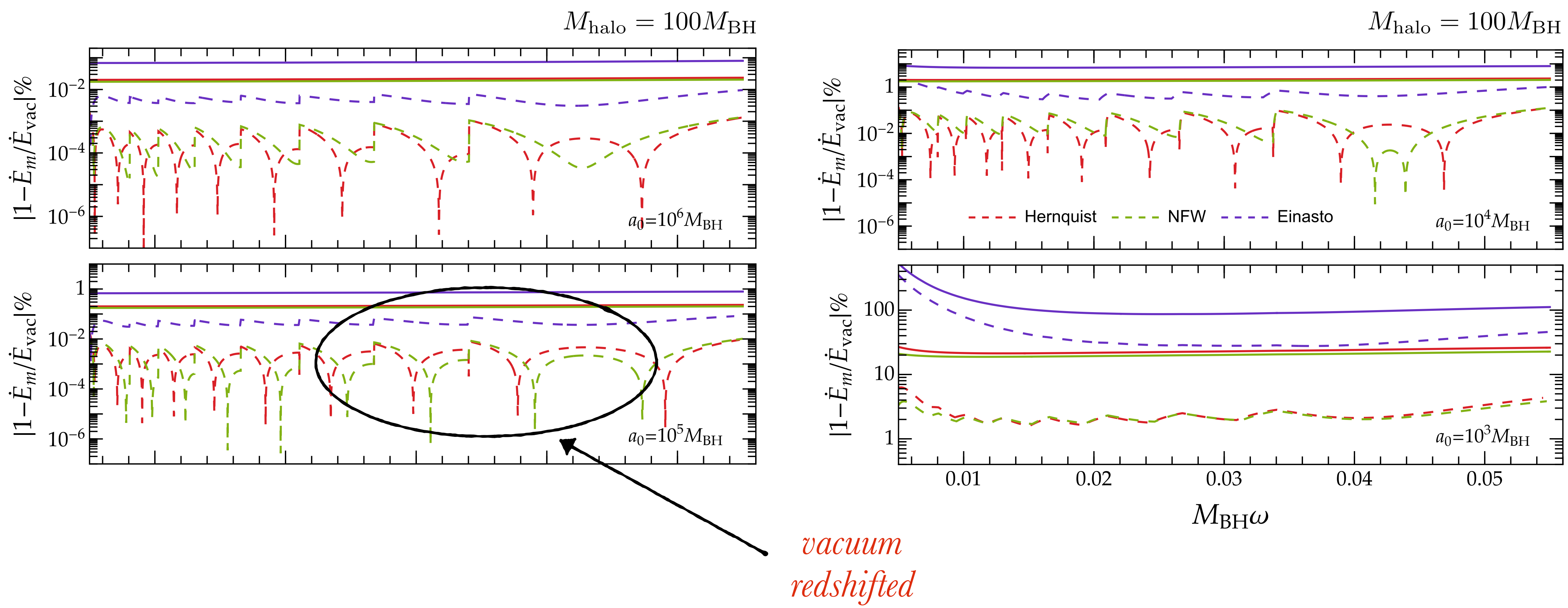

- Changes of axial fluxes can all be interpreted and quantified in terms of redshift scalings

- Redshifted quantities drastically reduce the difference for realistic halos

Polar modes

Polar sector introduces couplings between matter and metric components

- System of 5 coupled differential equations for $\vec{V} = (H_1, H_0, K, W, \delta\rho)$

$$\frac{d\vec{V}}{dr} = \mathbf{A}\vec{V} = \vec{S}$$

- The radial/tangential speeds of sound enter the modes

$$\delta p_{r,\ell m} = c_{s_r}^2 \delta\rho_{\ell m}$$
$$\delta p_{t,\ell m} = c_{s_t}^2 \delta\rho_{\ell m}$$

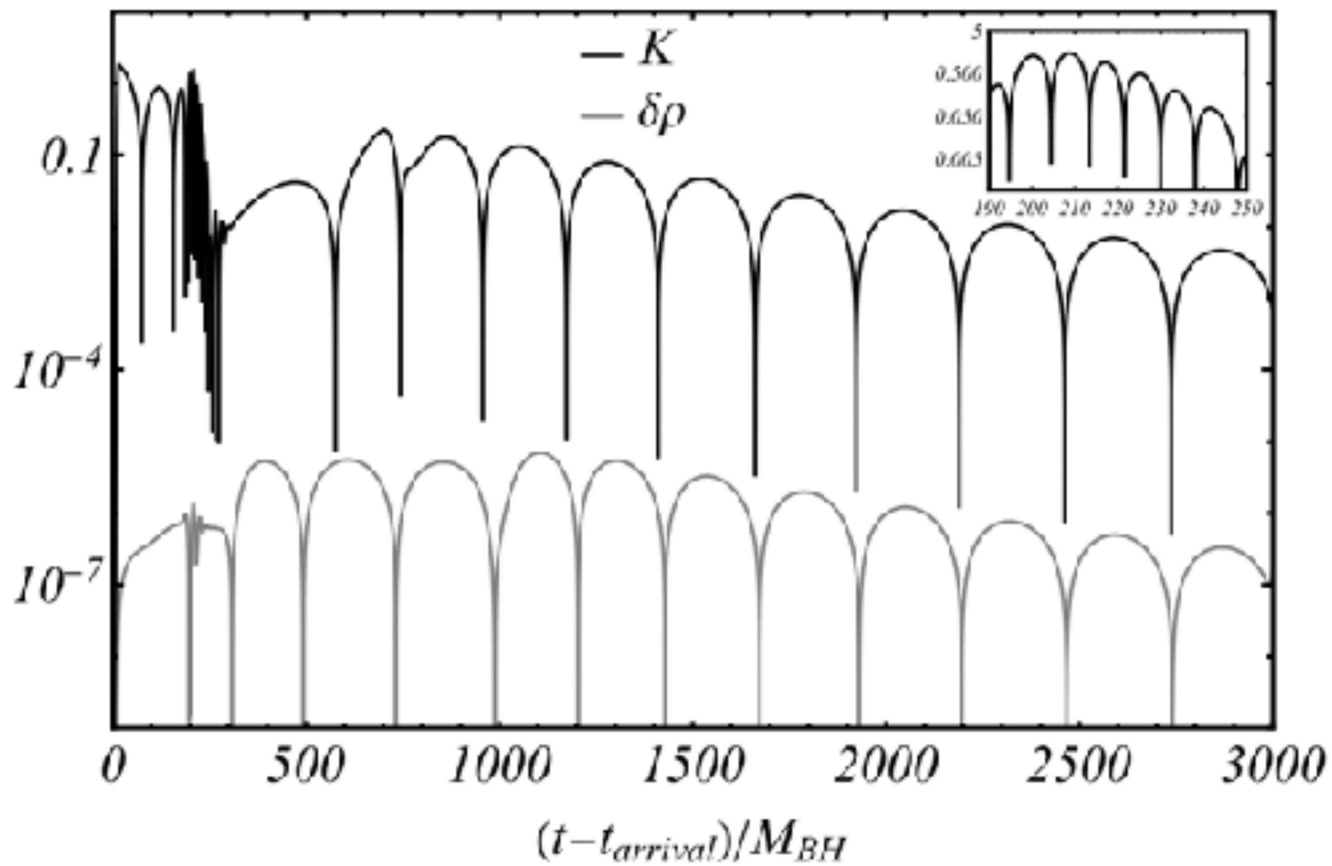

conversion between metric and fluid modes

Polar modes

(2,2) polar flux emitted by an EMRI on circular motion

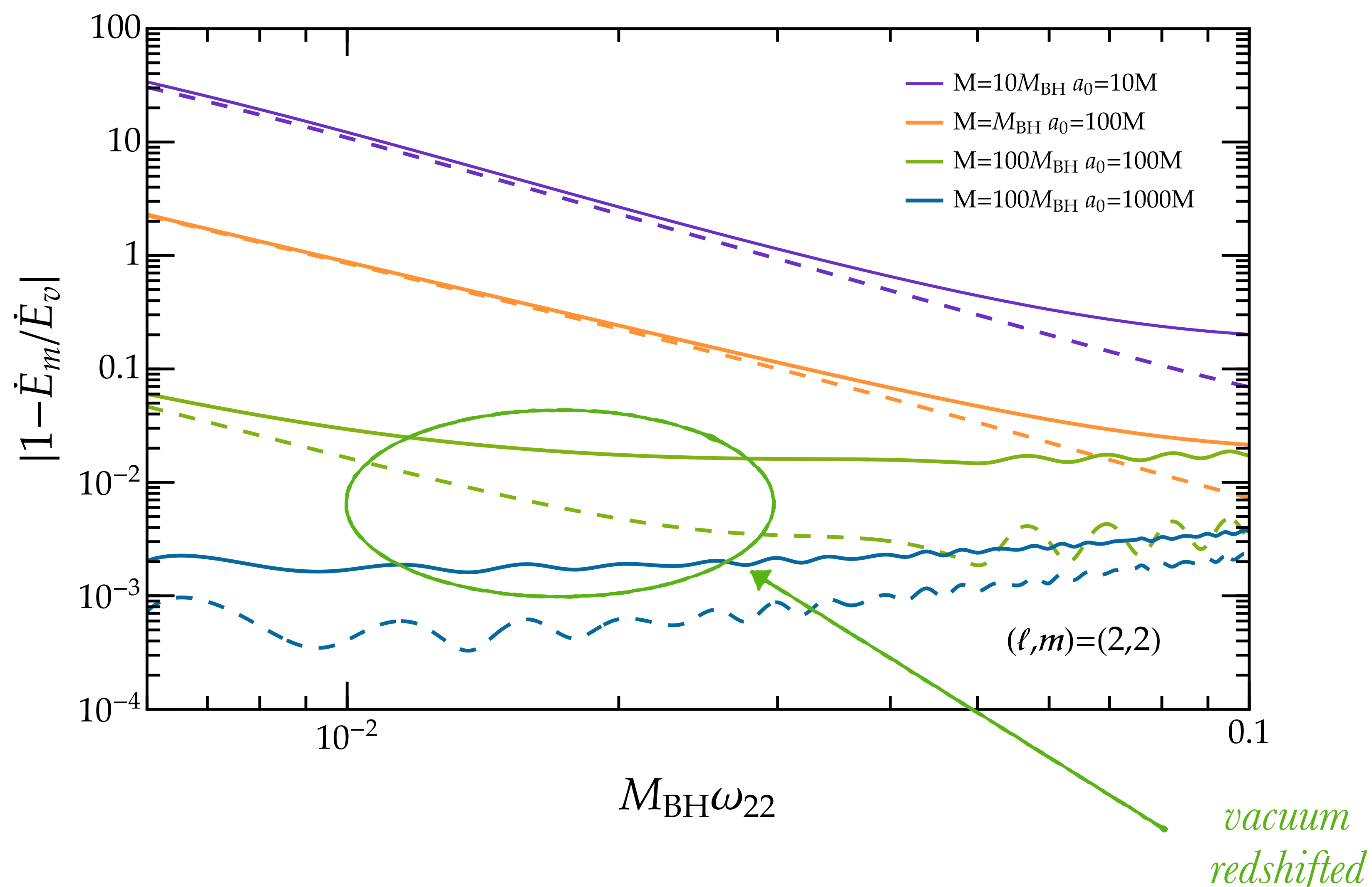

- Redshift rescaling not enough to take into account shift in the fluxes

- generation and propagation affected by deviations due to the coupling between polar modes and the fluid

Catching the dusty environment

S. Gliorio +, in preparation

$$\frac{dr}{dt} = -\dot{E}_{\rm GW}\frac{dr}{dE_{\rm orb}} \qquad \frac{d\Phi}{dt} = \sqrt{\frac{M}{r^3}} \xrightarrow{\textit{GW dephasing}} \Delta\Phi = \Phi_v - \Phi_m$$

$$\Delta\Phi \gtrsim 1 \longrightarrow$$ *evolution* <u>*can*</u> *be distinguishable*

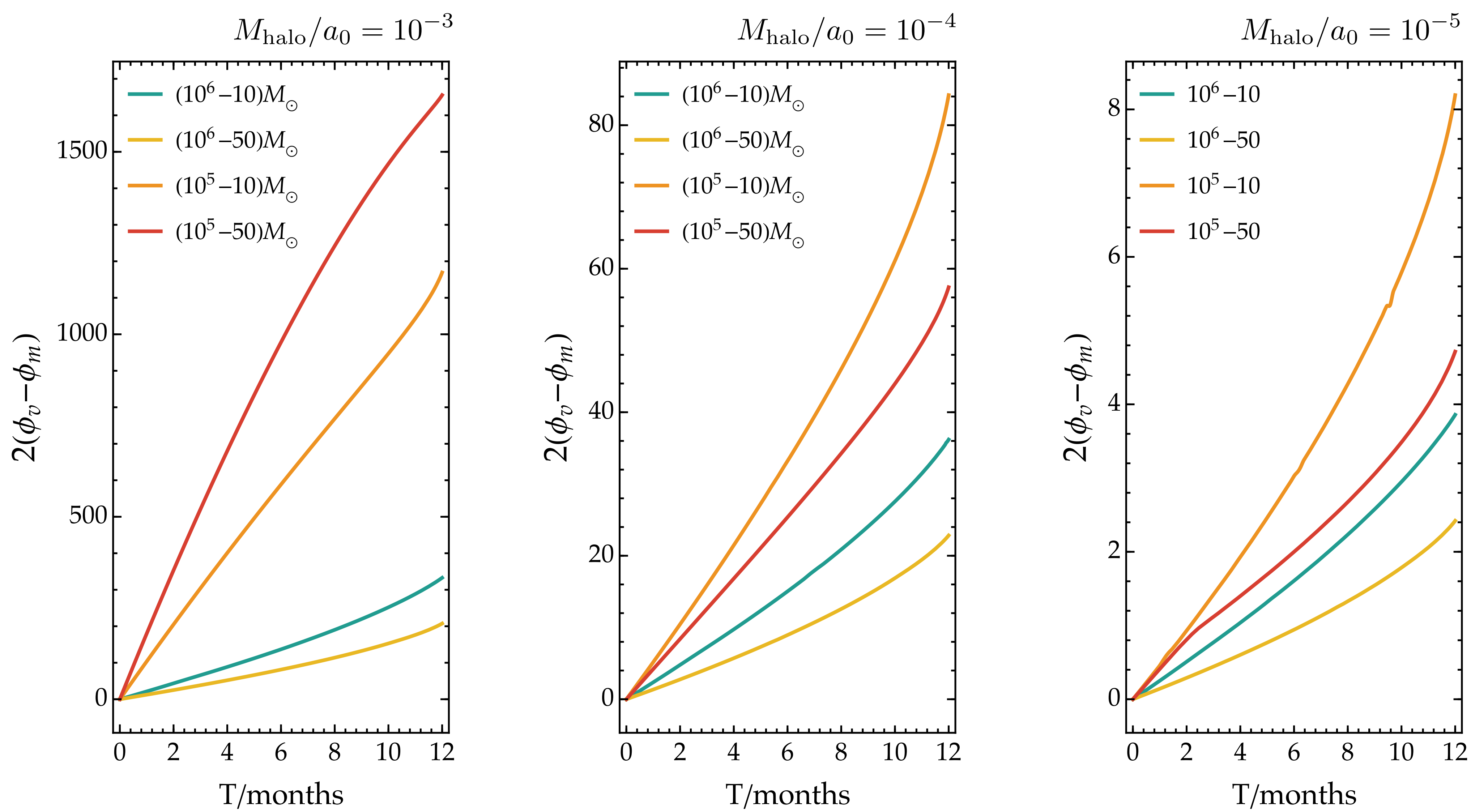

Distinguishing dusty waveforms

How different are vacuum and matter waveforms as seen by LISA ?

$$\langle h_v | h_m \rangle = 4\mathrm{Re} \int \frac{\tilde{h}_v(f)\tilde{h}_m(f)}{S_n(f)} df \longrightarrow \mathcal{F}[h_v, h_m] = \frac{\langle h_v | h_m \rangle}{\sqrt{\langle h_v | h_v \rangle \langle h_m | h_m \rangle}}$$

$\mathcal{F} \lesssim 0.997$ $\longrightarrow$ *signals may be distinguishable*

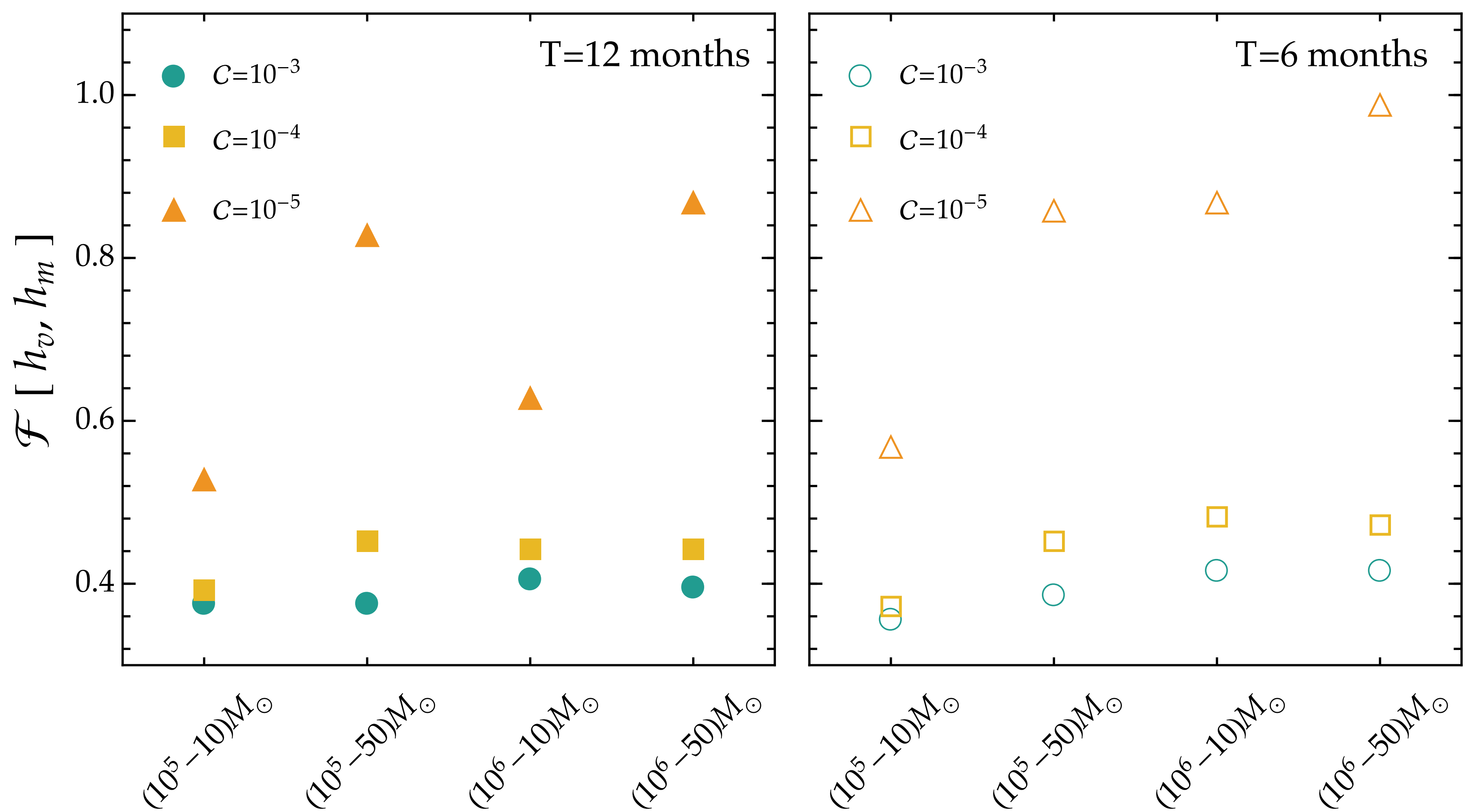

Back up

EMRIs in vacuum

How do we study EMRI in vacuum (GR)?

- The asymmetric character introduces a natural parameter to study the problem in perturbation theory $q = m_p/M \ll 1$

$$g_{\alpha\beta} = g^{(0)}_{\alpha\beta} + h_{\alpha\beta}$$

$$G_{\mu\nu} = T^{\mathrm{p}}_{\mu\nu} = 8\pi m_{\mathrm{p}} \int \frac{\delta^{(4)}(x - y_p(\lambda))}{\sqrt{-g}} \frac{dy_p^\alpha}{d\lambda} \frac{dy_p^\beta}{d\lambda} d\lambda \xrightarrow[\text{adiabatic}]{\text{leading}}$$

Regge-Wheeler-Zerilli
(Schwarzschild background)

Teukolsky
(Kerr background)

- The solution determines the phase evolution

$$\phi(t) = \underbrace{\phi_{\text{diss}-1}}_{\mathcal{O}(1/q)}^{\textit{adiabatic}} + \underbrace{\ldots}_{\mathcal{O}(1)}^{\textit{first post-adiabatic}} \xleftarrow[\ll 1 \textit{ radian}]{\textit{error}} \textit{needed}$$

EMRIs in vacuum

$$\mathbf{g}_{\alpha\beta} = g^{(0)}_{\alpha\beta} + q h^{(1)}_{\alpha\beta} + q^2 h^{(2)}_{\alpha\beta} + \mathcal{O}(q^3)$$

Contributions to the orbital trajectory

$$\frac{D^2 z^\alpha}{d\tau^2} = q f_1^\alpha + q^2 f_2^\alpha + \mathcal{O}(q^3)$$

Inspiral evolution on radiation-reaction time t_{rr}

$$t_{rr} = \mathcal{E}/\dot{\mathcal{E}} \sim M/q \xrightarrow[\text{of second order SF}]{\text{cumulative shift}} \delta z^\alpha \sim q^2 f_2^\alpha t_{rr}^2 \sim q^0$$

- Match filtering require error in phase << 1 radian: f_2^α f_3^α

$$\Phi(t) = \frac{1}{q}\left[\Phi_0(t) + q\Phi_1(t) + \mathcal{O}(q^3)\right]$$

$f^\alpha_{1,\mathrm{diss}}$ $f^\alpha_{1,\mathrm{cons}}$ $f^\alpha_{2,\mathrm{diss}}$

T. Hinderer & E. Flanagan, PRD 78, 064028 (2008)

A relativistic spacetime

Relativistic BH spacetime surrounded by a matter distribution

V. Cardoso +, PRD Lett. 105, L061501, (2022)
V. Cardoso +, PRL 129, 241103, (2022)
E. Figueiredo +, PRD 107, 104033, (2023)
N. Speeney +, PRD 109, 104079, (2024)

- Spherical symmetry + anisotropic stress energy tensor

$$ds^2 = -a(r)\,dt^2 + \frac{dr^2}{1-2m(r)/r} + r^2 d\Omega^2$$

$$\langle T^{\mu\nu}\rangle = \frac{n}{m_p}\langle P^\mu P^\nu\rangle \longleftrightarrow T^\mu{}_\nu = \mathrm{diag}(-\rho, 0, p_t, p_t)$$

A. Einstein, Annals Math. 40 (1939)

- Numerical solution for BHs in DM rich environments

average density *typical scale*

$$\rho(r) = \rho_0 (r/a_0)^{-\gamma}[1+(r/a_0)^\alpha]^{(\gamma-\beta)/\alpha} \qquad \rho(r) = \rho_e \exp\left\{-d_n[(r/r_e)^{1/n}-1]\right\}$$

Hernquist *NFW* *Einasto*

- Model characterised by M, a_0

The perturbation scheme

For the gravitational sector

$$h_{\alpha\beta} = h^{\rm pol}_{\alpha\beta} + h^{\rm ax}_{\alpha\beta}$$

$$(-1)^{\ell} \qquad\qquad (-1)^{\ell+1}$$

$$\mathbf{h} = \sum_{\ell=0}^{\infty}\sum_{m=-\ell}^{\ell} \boxed{\mathcal{A}^{(0)}_{\ell m}\mathbf{a}^{(0)}_{\ell m} + \mathcal{A}^{(1)}_{\ell m}\ \mathbf{a}^{(1)}_{\ell m} + \mathcal{A}_{\ell m}\mathbf{a}_{\ell m} + \mathcal{B}^{(0)}_{\ell m}\ \mathbf{b}^{(0)}_{\ell m} + \mathcal{B}_{\ell m}\ \mathbf{b}_{\ell m}} + \boxed{\mathcal{Q}^{(0)}_{\ell m}\ \mathbf{c}^{(0)}_{\ell m} + \mathcal{Q}_{\ell m}\ \mathbf{c}_{\ell m}}$$
$$\boxed{+\mathcal{D}_{\ell m}\ \mathbf{d}_{\ell m}} + \boxed{\mathcal{G}_{\ell m}\ \mathbf{g}_{\ell m} + \mathcal{F}_{\ell m}\ \mathbf{f}_{\ell m}\ .}$$

$$\mathbf{b}_{\ell m} = \frac{n_\ell r}{\sqrt{2}}\begin{pmatrix} 0 & 0 & 0 & 0 \\ 0 & 0 & Y^{\ell m}_{,\theta} & Y^{\ell m}_{,\phi} \\ 0 & Y^{\ell m}_{,\theta} & 0 & 0 \\ 0 & Y^{\ell m}_{,\phi} & 0 & 0 \end{pmatrix}$$

- 7 polar components + 3 axial harmonics
  - For a spherically symmetric background the 2 families decouple
  - In vacuum GR using the Regge-Wheeler-Zerilli gauge the components reduce to 1 axial and 1 polar functions

Regge & Wheeler, PRD 108, 1063 (1957)
Zerilli, PRD 2, 2141 (1970)

The wave equations

2 master equations for 2 perturbations

$$e^{-\lambda} = 1 - 2M/r$$
$$\Lambda = \ell(\ell+1)/2 - 1$$

$$\frac{d^2 R_{\ell m}}{dr_\star^2} + \left[\omega^2 - e^{-\lambda}\left(\frac{\ell(\ell+1)}{r^2} - \frac{6M}{r^3}\right)\right] R_{\ell m} = J_{\rm ax}$$

info on the orbital setup

Regge-Wheeler

$$\frac{d^2 Z_{\ell m}}{dr_\star^2} + \left[\omega^2 - \frac{18M^3 + 18M^2 r\Lambda + 6Mr^2\Lambda^2 + 2r^3\Lambda^2(1+\Lambda)}{r^3(3M + r\Lambda)}\right] Z_{\ell m} = J_{\rm pol}$$

Zerilli

- Perturbations are need to compute the GW fluxes…

$$\dot{E}^{\pm}_{\rm grav} = \frac{1}{64\pi}\sum_{\ell=2}^{\infty}\sum_{m=-\ell}^{\ell}\frac{(\ell+2)!}{(\ell-2)!}(\omega^2|Z^{\pm}_{\ell m}|^2 + 4|R^{\pm}_{\ell m}|^2)$$

- … which drive the orbital evolution

orbital phase

orbital radius

$$\frac{dr(t)}{dt} = -\dot{E}\frac{dr}{dE_{\rm orb}} \quad , \quad \frac{d\Phi(t)}{dt} = \frac{M^{\frac{1}{2}}}{r_p^{3/2}}$$

Polar modes

Polar sector introduces couplings between matter and metric components

- System of 5 coupled differential equations for $\vec{V} = (H_1, H_0, K, W, \delta\rho)$

$$\frac{d\vec{V}}{dr} = \mathbf{A}\vec{V} = \vec{S}$$

- The radial/tangential speeds of sound enter the modes

$$\delta p_{r,\ell m} = c_{s_r}^2 \delta\rho_{\ell m}$$
$$\delta p_{t,\ell m} = c_{s_t}^2 \delta\rho_{\ell m}$$

- (2,2) flux for secondary at $r_p \simeq 8M_{\rm BH}$

ℓ m	Vacuum		Hernquist	
		$\frac{M_{\rm Halo}}{a_0}$ \ $\frac{M_{\rm Halo}}{M_{\rm BH}}$	0.1	0.001
2 2	1.7068e-4	1	2.4341e-4	1.7038e-4
		100	1.4133e-4	1.7037e-4

less compact

the halo is diluted

the density is low close to the particle orbit

for a fixed compactness, a_0 increases for larger $M_{\rm Halo}$

more compact

Quasi Normal Modes

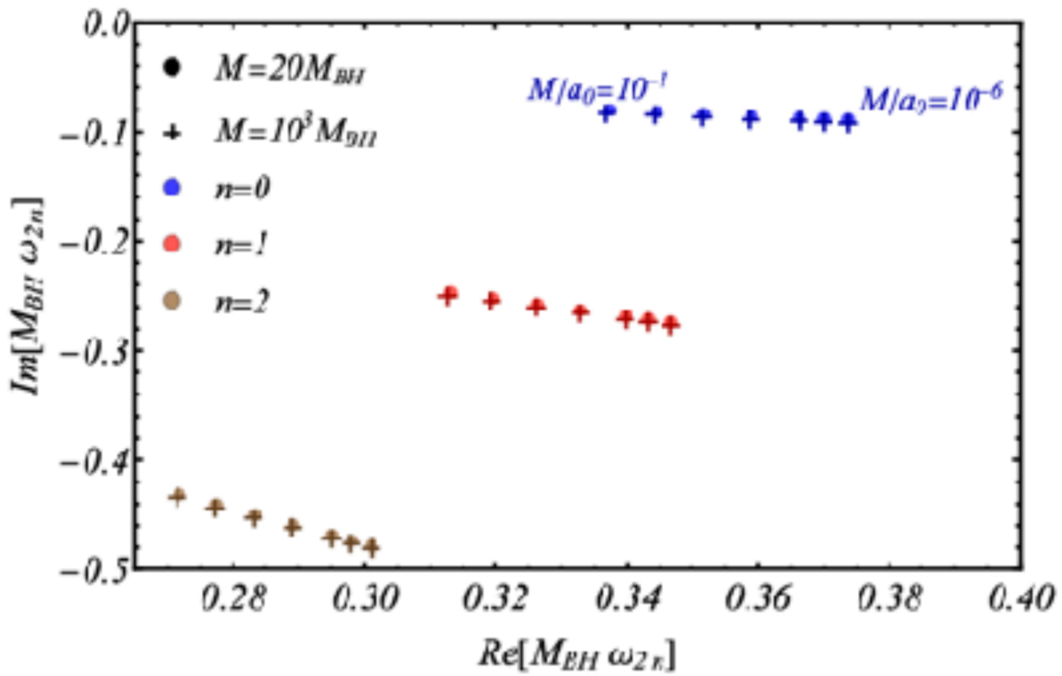

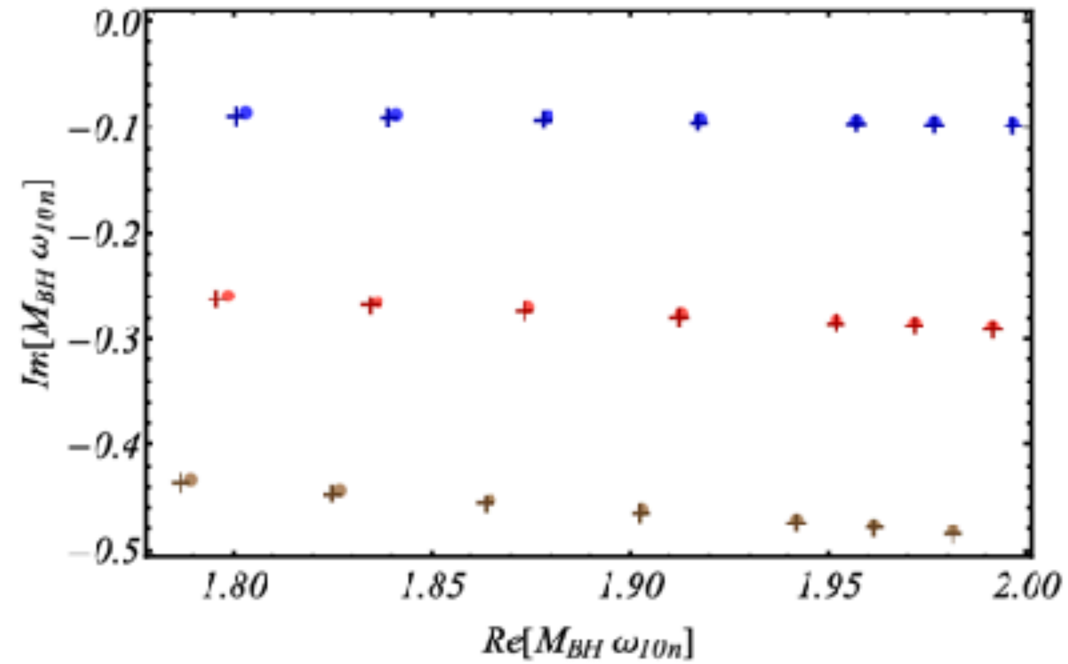

- Both real and imaginary part decrease as M/a_0 increases

redshift

effect

- Very little dependence on the halo mass
- In the eikonal limit $\omega_{\rm QNM} = \Omega_{\rm LR}\ell - i(n+1/2)|\lambda|$
- For small compactness

$$\frac{\Omega_{\rm LR}}{\Omega_{\rm LR}^{\rm vac}} \simeq 1 - \frac{M}{a_0} - 0.17\frac{M^2}{a_0} \qquad \frac{\lambda}{\lambda^{\rm vac}} \simeq 1 - \frac{M}{a_0} - 0.17\frac{M^2}{a_0}$$

Quasi Normal Modes

QNM behaviour as a function of the halo compactness

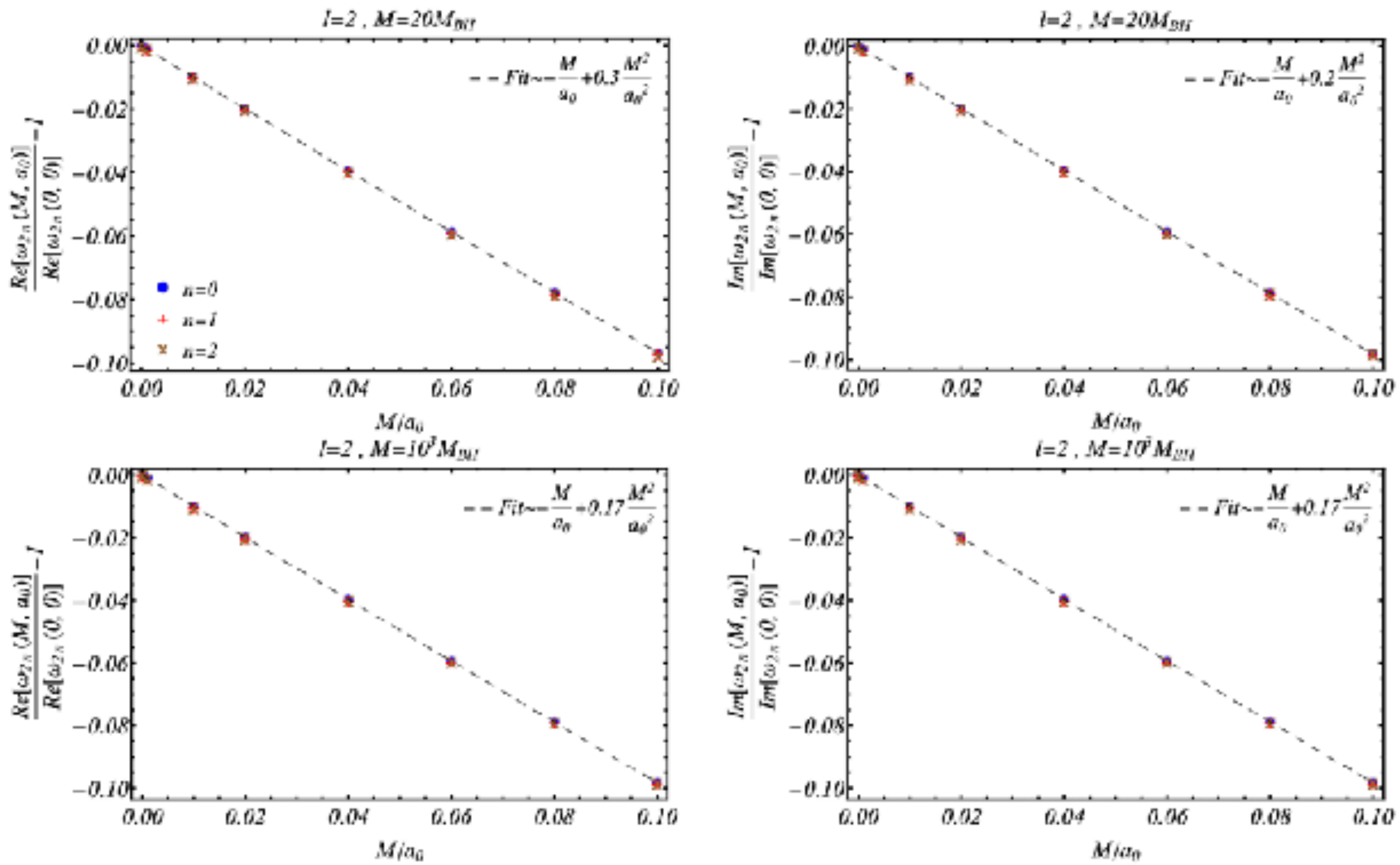

- The QNMs have a clear light-ring interpretation
- Linear and subdominant corrections agree with the analytic scaling of frequencies and damping times